A 920-Kilometer Optical Fiber Link for Frequency Metrology at the 19th Decimal Place

K. Predehl *et al.*

Science **336**, 441 (2012);
DOI: 10.1126/science.1218442

Science (print ISSN 0036-8075; online ISSN 1095-9203) is published weekly, except the last week in December, by the American Association for the Advancement of Science, 1200 New York Avenue NW, Washington, DC 20005.

A 920-Kilometer Optical Fiber Link for Frequency Metrology at the 19th Decimal Place

K. Predehl,[1]* G. Grosche,[2,3]† S. M. F. Raupach,[2]† S. Droste,[1] O. Terra,[2]‡ J. Alnis,[1] Th. Legero,[2] T. W. Hänsch,[1,4] Th. Udem,[1] R. Holzwarth,[1,5] H. Schnatz[2,3]

Optical clocks show unprecedented accuracy, surpassing that of previously available clock systems by more than one order of magnitude. Precise intercomparisons will enable a variety of experiments, including tests of fundamental quantum physics and cosmology and applications in geodesy and navigation. Well-established, satellite-based techniques for microwave dissemination are not adequate to compare optical clocks. Here, we present phase-stabilized distribution of an optical frequency over 920 kilometers of telecommunication fiber. We used two antiparallel fiber links to determine their fractional frequency instability (modified Allan deviation) to 5×10^{-15} in a 1-second integration time, reaching 10^{-18} in less than 1000 seconds. For long integration times τ, the deviation from the expected frequency value has been constrained to within 4×10^{-19}. The link may serve as part of a Europe-wide optical frequency dissemination network.

With residual fractional uncertainties at the 10^{-18} level (*1*), modern atomic frequency standards constitute extremely precise measurement devices. Besides frequency and time metrology, these standards provide valuable tools to investigate the validity of Einstein's theory of general relativity, to test the constancy of fundamental constants, and to verify predictions of quantum electrodynamics (*2*–*5*). Furthermore, geodesy, satellite navigation, and very long baseline interferometry may benefit from steadily improving precision of both microwave and optical atomic clocks (*6*).

Clocks ticking at optical frequencies slice time into much finer intervals than do microwave clocks and thus provide increased resolution. Eventually, this will result in a redefinition of the second in the International System of Units (SI) (*7*).

Characterizing a clock requires its comparison with one or more (ideally more) precise clocks. Unfortunately, the most precise optical clocks cannot be readily transported for comparison with one another.

Hence, to link the increasing number of worldwide precision laboratories, a suitable infrastructure is of crucial importance. The stabilities of current satellite-based dissemination techniques that use global satellite navigation systems [such as Global Positioning System, Global Navigation Satellite System (GLONASS), and GALILEO] or two-way satellite time and frequency transfer reach a fractional uncertainty level of the frequency of 10^{-15} after 1 day of comparison (*8*). Whereas this is sufficient for the comparison of most microwave clock systems, the exploitation of the full potential of optical clocks requires more advanced techniques (fig. S1).

We demonstrate that optical fiber networks can provide highly accurate means for long-distance clock comparisons. Frequency dissemination via fiber networks has so far been investigated over regional distances with the use of three different methods for transmission: (i) stable microwave frequency transfer by means of an amplitude-modulated laser (*9*), (ii) combined transfer of radio frequency and optical signals derived from an optical frequency comb (*10*), and (iii) transmission of an optical carrier wave of a stable continuous wave (cw) laser system (*11*–*13*). The transmission of an optical carrier wave provides the femtosecond resolution adapted to the accuracy of optical clocks. A cw laser signal is best suited to be transmitted over large distances, as it does not require dispersion compensation and is less sensitive to polarization mode dispersion. The transmission of optical carrier frequencies via stabilized urban fiber links of up to 172 km has been shown to have residual instabilities of a few parts in 10^{16} after 1-s linear decreasing with the inverse integration time τ (*14*–*16*). The longest fiber link investigated thus far had a total length of 480 km (*17*). The lowest fractional uncertainty of an optical signal transmitted over 146 km has been reported to be 1×10^{-19} (*15*). Real-time comparison of two strontium optical clocks has been demonstrated over a distance of 120 km with the use of optical telecommunication links (*18*).

[1]Max-Planck-Institut für Quantenoptik, Hans-Kopfermann-Strasse 1, 85748 Garching, Germany. [2]Physikalisch-Technische Bundesanstalt, Bundesallee 100, 38116 Braunschweig, Germany. [3]QUEST, Cluster of Excellence, Leibniz Universität, Welfengarten 1, 30167 Hannover, Germany. [4]Department of Physics, Ludwig-Maximilians Universität, Schellingstrasse 4, 80799 München, Germany. [5]Menlo Systems GmbH, Am Klopferspitz 19a, 82152 Martinsried, Germany.

*To whom correspondence should be addressed. E-mail: kdp@mpq.mpg.de

†These authors contributed equally to this work.

‡Present address: National Institute for Standards, Giza, Egypt.

Location	Length [km]	Attn. [dB]	Delay [ms]
PTB	0	0	0
Ammensleben	92	22	0.45
Cörmigk	79	21	0.39
Leipzig	114	24	0.56
Zimmritz	119	25	0.58
Großbreitenb.	79	20	0.45
Ebersdorf	74	19	0.36
Erlangen	102	23	0.50
Beilngries	88	19	0.43
Münchsmünster	82	18	0.40
MPQ	87	21	0.43
tot.	916	212	4.55

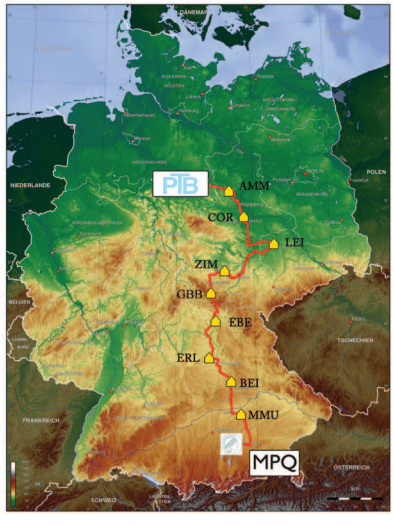

Fig. 1. Map of Germany with geographic locations of all access points, distance between access points, attenuation, and signal delay along the ~920-km fiber link connecting MPQ and PTB.

We used two 920-km-long fibers, F1 and F2, to connect the Max-Planck-Institut für Quantenoptik (MPQ) in Garching, Germany, and Physikalisch-Technische Bundesanstalt (PTB) in Braunschweig, Germany, which are separated by a geographical distance of 600 km (see Fig. 1). The fibers run in a cable conduit next to an underground gas pipeline.

Random changes of the optical path length due to acoustic noise and temperature fluctuations limit the stability and accuracy of the transmitted frequency. In our case, this results in fractional frequency excursions of ~5×10^{-14}. Active noise compensation is thus a prerequisite for stable and accurate transmission. This compensation is based on actively controlling the optical frequency entering the fiber link with an acousto-optic frequency shifter (*19*), where the link forms the long arm of a Michelson interferometer. Details and fundamental limitations are discussed in (*11*, *20*).

Over short distances, signal regeneration is not a critical issue and may be achieved without further in-line amplification (*12*, *14*). In our case, the inherent attenuation of 0.23 dB/km adds to a total one-way attenuation of more than 200 dB. Hence, nine pairs of carefully adjusted Erbium-doped fiber amplifier (EDFA) systems with low noise are distributed in repeater stations over the entire link length (Fig. 1). As the phase stabilization requires identical optical paths in both directions, all amplifiers are operated bidirectionally. In addition, we have implemented fiber Brillouin amplifiers (FBAs) with distributed gain (*17*) at both ends of the link, allowing coherent and fully transparent transmission. More details are given in (*20*).

Fiber links with the sender and receiver located in the same laboratory characterize the performance of the looped link but do not transfer a frequency between two remote users (*11*, *13*). In this work, we used two largely identical, but independent setups in an antiparallel configuration to comprehensively characterize the frequency transfer between the two institutes (Fig. 2). From each institute, we transmit a highly stable optical frequency (194 THz) f_{PTB} and f_{MPQ} to the other institute via two fibers F1 and F2. We measure $f_{F2} = f_{PTB} - f_{MPQ} + \delta f_{Laser} - \delta f_{LinkF2}$ at PTB, and $f_{F1} = f_{PTB} - f_{MPQ} + \delta f_{Laser} + \delta f_{LinkF1}$ at MPQ and calculate $\Delta f = f_{F2} - f_{F1}$.

With this antiparallel link configuration that is equivalent to a virtual loop, the noise δf_{Laser} of both lasers cancels in the difference of the two beat notes, whereas the noise δf_{Link} of both fibers adds. Hence, we derive an upper limit for the residual instability and uncertainty of the transmitted frequency.

Due to slow drifts of the stable lasers used on both sides, any timing offset between the frequency counters at PTB and MPQ resulting from imperfect synchronization leads to a frequency shift between the two signals $f_{F1}(t)$ and $f_{F2}(t)$. Without correction, this shift would contribute with a systematic fractional uncertainty of ~1.5×10^{-16}. We determined the timing offset before each measurement by modulating one of the lasers (*20*). After correction, this timing offset contributes with less than three parts in 10^{19}.

We used dead-time free, high-resolution frequency counters operating in a nonaveraging (Π-type) or an averaging (Λ-type) mode (*21*) with a 1-s gate time to record $f_{F1}(t)$ and $f_{F2}(t)$. Fully redundant counting (*22*) allows us to detect possible loss of phase coherence (cycle slip) arising from a deteriorated signal-to-noise ratio. We evaluated data only for periods with no cycle slips. Under optimized conditions, the rate of cycle slips is as low as a few per day, and the signal phase can be continuously tracked for several hours. Routine operation over several days requires regular adjustment of the polarization.

In Figure 3, we show the overlapping Allan deviation (ADEV) (*23*) for the unstabilized and stabilized link when measured with Π-type counters. The fractional instability of 3.8×10^{-14} s τ^{-1} of the stabilized link shown in Fig. 3 for a 35000-s-long data set is due to the residual broadband fiber noise. The ADEV drops off as τ^{-1}, as expected for a phase-stabilized fiber link. The observed instability agrees superbly with the theoretical

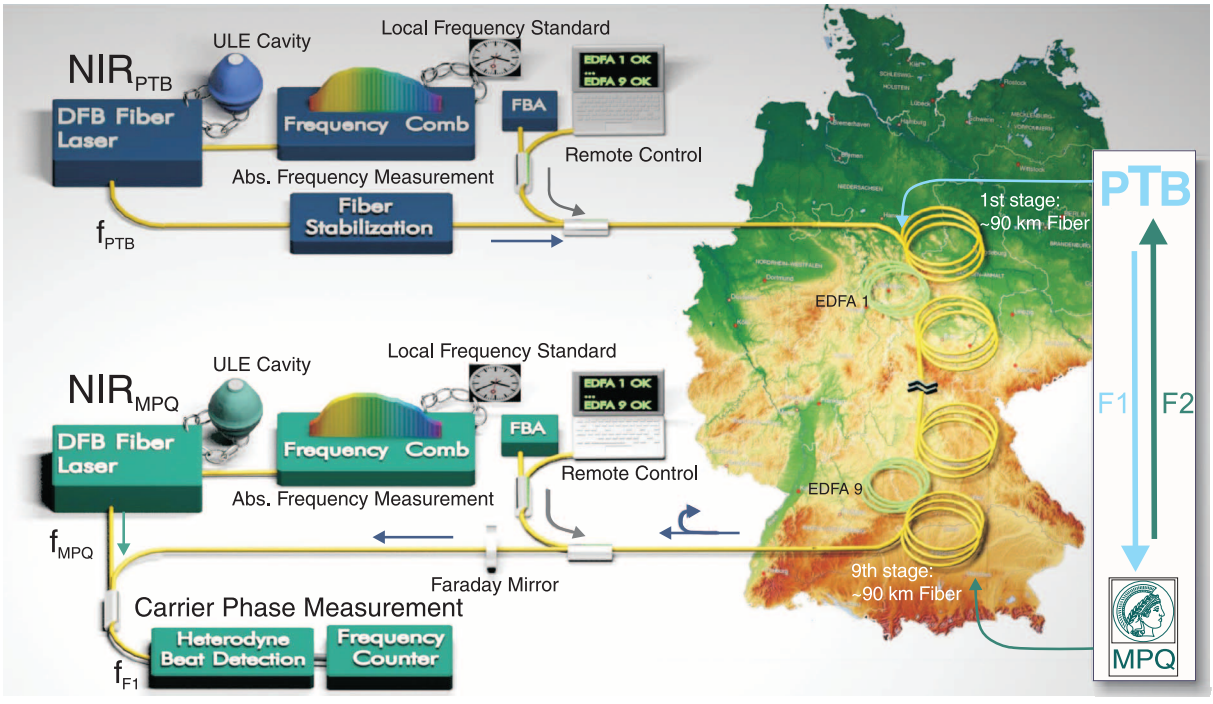

Fig. 2. Experimental setup for the characterization of two 920-km fiber links (for clarity, only one fiber is shown). Fiber F1 is used to transmit an optical frequency f_{PTB} of a distributed feedback (DFB) fiber laser (NIR_{PTB}) to MPQ. The laser operates at a frequency of 194 THz (~1542 nm). It shows a linewidth of a few hertz and a residual drift of ~100 mHz/s when locked to a high-finesse cavity made out of ultralow-expansion glass (ULE). Thus, short-term laser noise becomes negligible compared with the phase noise of the free-running fiber link (*19*). By means of a femtosecond comb (*25*), the laser's frequency is measured against the local microwave standard. F1 is actively stabilized in a single step and further equipped with 11 optical amplifier systems (remotely controlled EDFAs and FBAs) to preserve the signal power and coherence. To avoid stimulated Brillouin scattering, we limit the power launched into the fibers to 6 mW. At MPQ, a heterodyne beat note f_{F1} between f_{MPQ} and f_{PTB} is measured. Likewise, we transmit f_{MPQ} via fiber F2 from MPQ to PTB and generate a beat note f_{F2}.

prediction in (*15*), thus providing strong confirmation of the $L^{3/2}$ scaling law derived in (*11*), for distances up to 1000 km.

To demonstrate the link's instability floor and illustrate the potential of adapting the type of averaging to the dominant noise type, we additionally show data, where the counters were operated in Λ mode (overlapping weighted average). As shown in Fig. 3 for a 18000-s-long data set, we achieve a residual instability (modified ADEV) of 5×10^{-15} in 1 s. It averages as $\tau^{-3/2}$ for up to 100 s and reaches 10^{-18} in less than 15 min. The deviation of the fractional instability from the $\tau^{-3/2}$ slope for $\tau > 300$ s is mainly due to a few tens of centimeters of uncompensated fiber in the MPQ laboratory that have not been temperature-stabilized. We estimated the corresponding uncertainty for the MPQ interferometer to be $<3 \times 10^{-19}$ (*20*).

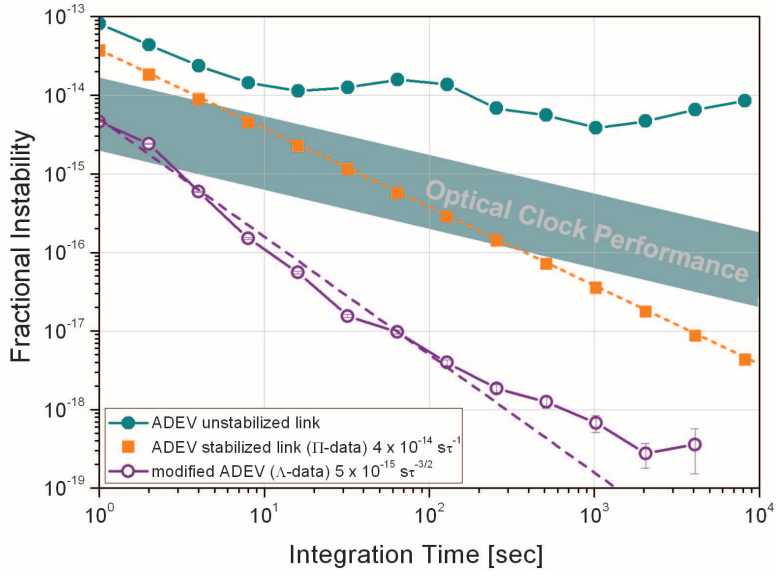

Fig. 3. Fractional instability of two 920-km telecom fiber links F1 and F2 connecting PTB and MPQ. We show the overlapping ADEV of the unstabilized link (solid circles) and stabilized link (squares) derived from a nonaveraging counter for a 35000-s-long data set. We also show the modified ADEV (open circles) for a 18000-s-long data set from data taken with averaging (Λ-type) counters, which allows us to distinguish white phase noise from flicker phase noise (*21*). The ADEV for state-of-the-art optical clock performances is depicted for comparison. The dashed lines indicate the expected stability curves for a signal dominated by white phase noise.

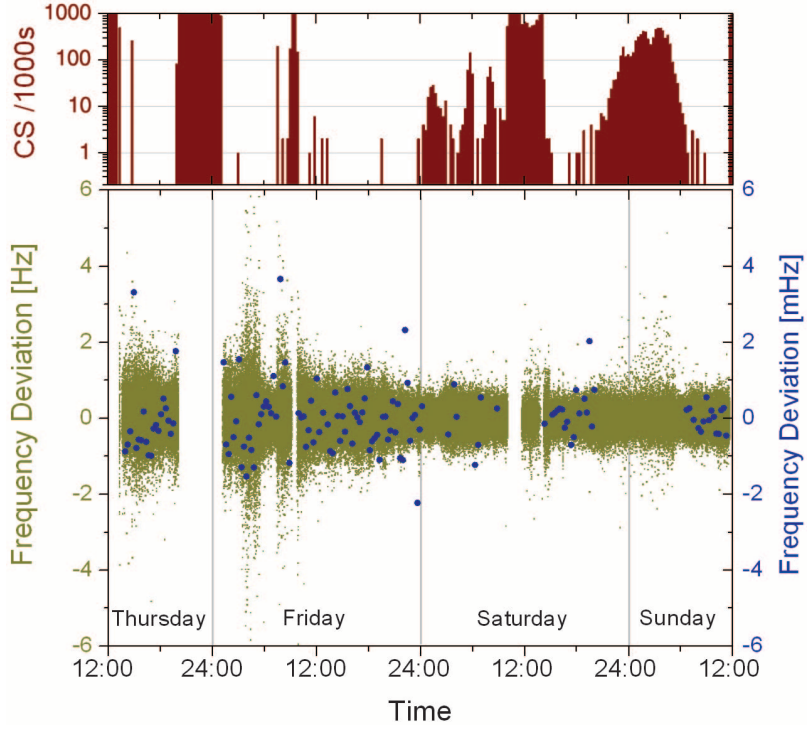

Fig. 4. Four-day frequency comparison between MPQ and PTB. Data are taken with high-resolution Λ-type frequency counters (overlapping triangle weighting, no dead time) with 1-s gate time (green data points, left frequency axis). Cycle slip (CS) rates per 1000 s are shown in the upper plot. Phase-coherent intervals have been binned into 1000-s-long sequences and averaged. From the 135 resulting data points (dark blue, right frequency axis, enlarged scale), we calculated a fractional deviation from the expected frequency of $(0.7 \pm 3.7) \times 10^{-19}$.

The accuracy of the transmitted signal might be compromised by systematic offsets that would not be observed in the instability analysis. From data taken with a Λ-type counter over a period of 4 days, we selected all continuous data subsets with a length of 1000 s, as shown in Fig. 4. The arithmetic mean of each subset is calculated to benefit from the strong suppression of white phase noise for longer integration times. The resulting 135 data points have a mean of 13 μHz and a SD σ = 823 μHz; more than 80% of the values are within 1σ (fig. S2). The statistical fractional uncertainty of the mean is 3.7×10^{-19}. Thus, we can constrain the deviations from the expected frequency value to be less than 4×10^{-19}. This value exceeds the requirements posed by the most accurate atomic clocks to date by more than one order of magnitude.

As a first application, we have used the fiber link to measure the 1*S*-2*S* two-photon transition frequency in atomic hydrogen at MPQ, using PTB's primary Cs-fountain clock (CSF1) as a reference (*24*). The hydrogen experiment constitutes a very accurate test bed for quantum electrodynamics and has been performed at MPQ with ever increasing accuracy. The latest measurement (*3*) has reached a level of precision at which satellite-based referencing to a remote primary clock would limit the experiment. As the transmission over fiber is up to three orders of magnitude more stable, a frequency measurement can be carried out straightforwardly without the need for transporting a frequency standard to the experiment.

The link now permanently connects MPQ and PTB and is operated routinely. Going beyond a proof-of-principle experiment conducted under optimized laboratory conditions, it constitutes a solution for the topical issue of remote optical-clock comparison, opening a variety of applications in fundamental physics, such as tests of general and special relativity as well as quantum electrodynamics. Furthermore, such a link will enable clock-based, relativistic geodesy at the subdecimeter level. Applications in navigation, geology, dynamic ocean topography, and seismology are currently being discussed. Some of

the future applications of optical clocks will be space-based, and their operation will require ground stations with access to ultrastable frequency references linked to the best available clocks. In this respect, optical links will become of central importance.

References and Notes

1. C. W. Chou, D. B. Hume, J. C. J. Koelemeij, D. J. Wineland, T. Rosenband, *Phys. Rev. Lett.* **104**, 070802 (2010).
2. C. W. Chou, D. B. Hume, T. Rosenband, D. J. Wineland, *Science* **329**, 1630 (2010).
3. C. G. Parthey *et al.*, *Phys. Rev. Lett.* **107**, 203001 (2011).
4. T. Rosenband *et al.*, *Science* **319**, 1808 (2008).
5. A. Shelkovnikov, R. J. Butcher, C. Chardonnet, A. Amy-Klein, *Phys. Rev. Lett.* **100**, 150801 (2008).
6. S. Schiller *et al.*, *Exp. Astron.* **23**, 573 (2009).
7. P. Gill, F. Riehle, *Proceedings of the 20th European Frequency and Time Forum*, Braunschweig, Germany, 27 to 30 March 2006.
8. A. Bauch *et al.*, *Metrologia* **43**, 109 (2006).
9. O. Lopez *et al.*, *Eur. Phys. J. D* **48**, 35 (2008).
10. G. Marra *et al.*, *Opt. Lett.* **36**, 511 (2011).
11. N. R. Newbury, P. A. Williams, W. C. Swann, *Opt. Lett.* **32**, 3056 (2007).
12. O. Terra *et al.*, *Appl. Phys. B* **97**, 541 (2009).
13. O. Lopez *et al.*, *Opt. Express* **18**, 16849 (2010).
14. M. Musha, F.-L. Hong, K. Nakagawa, K.-I. Ueda, *Opt. Express* **16**, 16459 (2008).
15. G. Grosche *et al.*, *Opt. Lett.* **34**, 2270 (2009).
16. H. Jiang *et al.*, *J. Opt. Soc. Am. B* **25**, 2029 (2008).
17. O. Terra, G. Grosche, H. Schnatz, *Opt. Express* **18**, 16102 (2010).
18. Yamaguchi *et al.*, *Appl. Phys. Express* **4**, 082203 (2011).
19. L. S. Ma, P. Jungner, J. Ye, J. L. Hall, *Opt. Lett.* **19**, 1777 (1994).
20. Materials and methods are available as supplementary materials on *Science* Online.
21. S. T. Dawkins, J. J. McFerran, A. N. Luiten, *IEEE Trans. Ultrason. Ferroelectr. Freq. Control* **54**, 918 (2007).
22. Th. Udem, J. Reichert, T. W. Hänsch, M. Kourogi, *Opt. Lett.* **23**, 1387 (1998).
23. W. J. Riley, *NIST Special Publication 1065* [National Institute of Standards and Technology (NIST), Boulder, CO, 2008].
24. S. Weyers, U. Hübner, R. Schröder, Chr. Tamm, A. Bauch, *Metrologia* **38**, 343 (2001).
25. G. B. Hocker, *Appl. Opt.* **18**, 1445 (1979).

Acknowledgments: We thank the members of Deutsches Forschungsnetz in Berlin, Leipzig, and Erlangen, Germany, as well as Gasline GmbH for a fruitful collaboration. We also thank the European Space Agency and the excellence cluster QUEST for financial support; A. Koczwara, N. Kolachevsky, U. Sterr, A. Thaller, and T. Wilken for experimental support and helpful discussions; F. Riehle for long-term encouragement; and B. Lipphardt for technical support. T.W.H. acknowledges support by the Max Planck Foundation.

Supplementary Materials

www.sciencemag.org/cgi/content/full/336/6080/441/DC1
Materials and Methods
Figs. S1 and S2
Reference (*26*)

27 December 2011; accepted 27 February 2012
10.1126/science.1218442

Revealing the Angular Symmetry of Chemical Bonds by Atomic Force Microscopy

Joachim Welker and Franz J. Giessibl*

We have measured the angular dependence of chemical bonding forces between a carbon monoxide molecule that is adsorbed to a copper surface and the terminal atom of the metallic tip of a combined scanning tunneling microscope and atomic force microscope. We provide tomographic maps of force and current as a function of distance that revealed the emergence of strongly directional chemical bonds as tip and sample approach. The force maps show pronounced single, dual, or triple minima depending on the orientation of the tip atom, whereas tunneling current maps showed a single minimum for all three tip conditions. We introduce an angular dependent model for the bonding energy that maps the observed experimental data for all observed orientations and distances.

When more than two atoms are involved, the forces that act between atoms generally depend not only on their distance but also on the angles between the atoms. Chemical bonds establish an equilibrium between attractive and repulsive interactions for atoms that is described by the Morse potential (*1*). When more than two atoms are involved, the bonding energy generally depends on the bonding angle as well as distance, and model potentials with an angular dependence, such as the Stillinger-Weber potential (*2*), are needed. The directional character of the atomic bonds is reflected in the crystal structure. Most metals condense in a face-centered cubic (fcc), hexagonal close-packed (hcp), or body-centered cubic (bcc) lattice (*3*). In particular, metals with unfilled p or d shells can show strong directional bonding [chapters 1.4 and 2.5 in (*3*)]. Although fcc and hcp lattices have the largest possible number of nearest neighbors, the angular dependence of atomic forces leads to slight energetic differences between fcc and hcp lattice structures. Atomic manipulation of cobalt atoms on a copper surface by scanning tunneling microscopy (STM) has shown that a Co adatom on a Cu(111) surface prefers to occupy an fcc site over an hcp site, although the adatom is in both cases sitting directly in a dip between three Cu atoms (*4*).

Atomic force microscopy (AFM) (*5*) can measure forces between individual atoms with great precision, and recent progress in three-dimensional force spectroscopy (*6*–*8*) helps to investigate the angular dependence of atomic bonding forces. Initial manifestations of an angular dependence of bonding forces led to the observation of subatomic features on the surface of Si (*9*). The data were explained by the directional dependence of covalent bonds between a Si tip with a Si adatom on the sample [figure 4 in (*9*)] as predicted by calculating the tip-sample interaction using the Stillinger-Weber potential (*2*), a classic model potential for diamond structure materials. Density functional theory (DFT) calculations by two groups (*10*, *11*) supported the covalent-bonding theory, but other authors (*12*) proposed that the data could have been the result of a feedback artifact, and there has been a recent theoretical proposal that the angular dependence could be caused by multiple-atom tips (*13*). Simultaneous STM and AFM experiments of a W tip imaging a graphite sample showed a single current maximum and multiple force maxima in the image of the W tip atom (*14*); hence, AFM can address electronic states that are spatially more confined than electronic states that are accessible to STM. In that experiment, the light and small carbon atoms have produced repeated images of the electronic valence states in tungsten atoms [see figures B and C in (*15*)]. Recent DFT calculations confirmed that the electronic structure of W should show these small features (*16*). However, the softness and close atomic packing of graphite make it difficult to calculate the experimental observables, and distance-dependent data were not available in the first experiments.

Precise measurements of the interaction of two single and clearly defined atomic bonding partners as a function of distance and angle would allow us to study the evolution of the atomic angular dependencies and provide well-defined experimental data that can serve as a reference for theoretical calculations. Here, we present an experimental study of the interaction of two well-defined bonding partners: a single CO molecule that is bonded to a Cu(111) surface and the metallic front atom of a tip. We analyzed tunneling current and frequency shift in three dimensions and were therefore able to recover the force and potential energy between two atomic bonding partners as a function of angle and distance.

We used STM (*17*) combined with frequency modulation AFM (*18*), where a quartz cantilever (qPlus sensor) (*19*) with a stiffness of k = 1800 N/m, an eigenfrequency of f_0 = 27275.20 Hz, a quality factor of Q = 195870, and a W tip oscillated with a constant amplitude A (here, we

Experimental and Applied Physics, University of Regensburg, 93053 Regensburg, Germany.

*To whom correspondence should be addressed. E-mail: franz.giessibl@ur.de